

PHOTO - ENHANCED RESISTANCE SWITCHING BEHAVIOUR IN (PEA)₂CuCl₄ 2-DIMENSIONAL PEROVSKITE

ANCY ALBERT

Currently Pursuing PhD program in Department of Physics in Amrita Vishwa Vidyapeetham, Amritapuri, India. E-Mail: ancy@am.amrita.edu

ABHITHA A B

Currently pursuing master's degree program, Department of Physics in Amrita Vishwa Vidyapeetham, Amritapuri, India. E-Mail: abhithashiva@gmail.com

C O SREEKALA

Assistant professor, Department of Physics, Amrita Vishwa Vidyapeetham, Amritapuri India. E-Mail: sreekalaco@am.amrita.edu

Abstract

The structural tunability and optical and thermal properties allured interest in hybrid perovskites. (PEA)₂CuCl₄ a lead-free 2D organic-inorganic hybrid perovskite of band gap 2.91eV, was synthesised, and its optical and electrical characterisations were reported in this work. The temperature-dependend optical characteristics show a shift in absorbance and transmittance, indicating the thermochromic nature of the material due to the non-rigid copper ion and subsequent Jahn-Teller distortion arising on heating. The morphological analysis confirmed uniformity of (PEA)₂CuCl₄ thin film. The structural analysis confirmed that the material belonged to an orthorhombic non-centrosymmetric crystal structure, and the hysteresis loop obtained in capacitance versus applied voltage characteristics supported the ferroelectric behaviour of the material. Current versus voltage characteristics of (PEA)₂CuCl₄ show resistance switching behaviour promising for memory device application. The switching behaviour was analysed in light and dark environments. The light environment enhanced resistance switching in the material.

Index Terms: C-V hysteresis loop, Copper halide perovskite, Island morphology, Non-centrosymmetric, Rietveld refinement, Resistance switching, Thermochromic properties.

1. INTRODUCTION

Halide perovskites show interesting physical properties such as high absorption coefficient, ambipolar charge transport, tunable band gap, low exciton binding energy, ferroelectricity, etc. [1-7]. Miyasaka et al. in 2009 applied methylammonium lead iodide (MAPbI₃) and methylammonium lead bromide (MAPbBr₃) perovskites to sensitise to TiO₂ (titanium dioxide) for visible light with maximum efficiency of 3.8% [8]. Later, in 2011 park et al. synthesised MAPbI₃ nanocrystals and applied them in the solar cell, which showed an efficiency of 6.5% [9]. Followed by these, a hand full of innovative works came out using halide perovskites in solar cells, light-emitting diodes (LEDs), photodetectors, memory devices, field effect transistors, batteries and piezoelectric energy harvesters [10-16]. Even though the material performs well, chemical instability and lead toxicity retract its mass commercialisation [17-19].

Stability was attained by developing 2-dimensional (2D) perovskites [20, 21]. Ruddelson-popper(RP) and Dion-Jacobson (DJ) are the two important types of 2D

perovskite structures, A_2MX_4 and AMX_3 respectively, where A is largely organic or inorganic cations (e.g.: MA^+ , FA^+ (formamidinium), Cs^+ (caesium), PEA^+ (phenyl ethyl ammonium) etc.) and M is the metallic smaller cation (Pb^{2+} , Sn^{2+} (tin), Cu^{2+} (copper) etc) and X is the halide anion $.Cl^{-1}$ (chloride), Br^{-1} , I^{-1} [22, 23]. Also, lead toxicity can be stamped out by replacing it with metallic cations such as Sn, bismuth (Bi), (Cu), germanium (Ge) etc. [24-27]. Cu-based halide perovskite is a better choice in this scenario because it forms a 2D environment-friendly perovskite [28, 29].

A number of Cu-based perovskite materials were reported to be flexible with temperature and light, showing thermochromism and photochromism [30, 31]. Non-rigid nature of Cu ion with electronic configuration $3d^9$ is responsible for this behaviour [32]. Li et al. reported the thermochromic behaviour of different Cu-based halide perovskites in smart windows [33]. B. G. H. M. Groeneveld et al. reported a photochromic phenomenon in 2D Cu-based perovskites [34]. Also, organic cations with phenyl ring showed high moisture stability compared to the commonly used methylammonium cation, which reported better performance [35, 36]. A. O. Polyakov et al. reported the coexistence of ferroelectricity and ferromagnetism in $(PEA)_2CuCl_4$ RP-perovskite. According to them, octahedral tilting and twisting in the structure of $(PEA)_2CuCl_4$ can naturally give rise to polarisation [37]. In this work, a stable $(PEA)_2CuCl_4$ 2D perovskite was synthesised, and its temperature-dependent optical characteristics, electrical characteristics and effect of photons on the resistance switching mechanism were studied.

2. EXPERIMENTAL SECTION

2.1 Materials used

phenyl ethyl amine (PEA) (99%, Sigma Aldrich), Copper (2) chloride ($CuCl_2$) (98%, Sigma Aldrich), con. Hydrochloric acid (HCl) (35% in distilled water, Merck), ethanol (99.8%, HI Media), N, N-Dimethylformamide (DMF) (99.9%, Merck) and distilled water, Fluorine doped tin oxide coated glass substrates (FTO glass substrate).

2.2. Methods

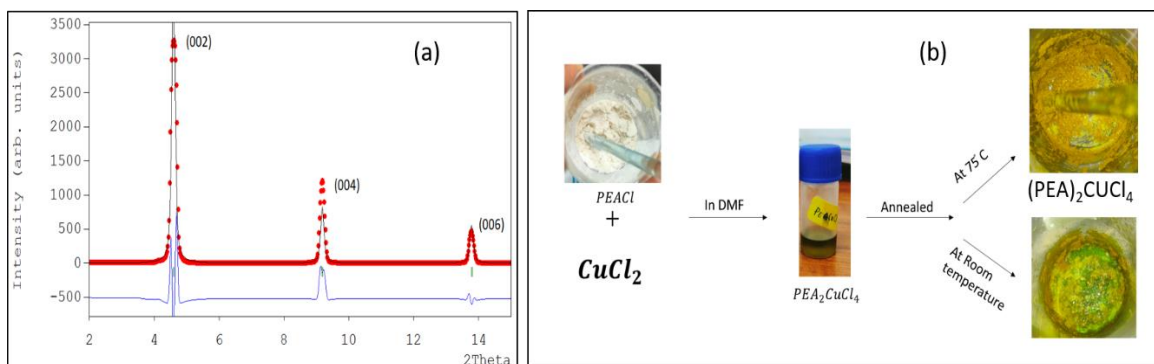
2 molar (M) solution of HCl and PEA were dissolved in distilled water and ethanol respectively and stirred at $0^\circ C$ for 40 minutes. Then, the acidic solution was added and dropped wisely into the PEA solution and stirred for 2 hours at $0^\circ C$. The solution was dried at $60^\circ C$ to obtain phenyl ethyl ammonium chloride (PEACl) powder. The powder was recrystallised two times to attain desired purity. The powder is stored in diethyl ether [38, 39]. 1.716g of PEACl and 0.67g of $CuCl_2$ (2:1 ratio) were dissolved in 10 ml DMF and stirred for 4 hours at $80^\circ C$ to get $(PEA)_2CuCl_4$. The solution was spin-coated (EZspinA1-spin coater) on FTO glass substrates at 2000 rpm for 40 seconds repeated the process 5 times.

Morphology of the prepared films was checked using Field Emission Scanning Electron Microscope (FE-SEM) (Gemini 300, Zeiss) and structural analysis was done using X-ray diffraction (XRD) facility (Rigaku Goniometer model ultima IV) at COE-AMGT respectively in Amrita Vishwa Vidyapeetham, India. Absorbance in the Ultra Violet (UV)-Visible (VIS) region was analysed using a Thermo Scientific Nicolet iS50 UV-VIS spectrometer at CLIF, University of Kerala, India. The films of $(\text{PEA})_2\text{CuCl}_4$ show a colour change from yellow to orange upon heating. This thermochromic behaviour was confirmed via temperature depended optical study done with the help of CARY 100 WIN UV-VIS spectrophotometer version: 4.20 (Agilent Technologies), NIPER Raebareli, India. Electrical characterisations to study photo-induced resistance switching was performed via the semiconductor parameter analyser, Keysight B1500A in IIT Palghat, India.

3. RESULTS AND DISCUSSION

3.1 Structural Analysis

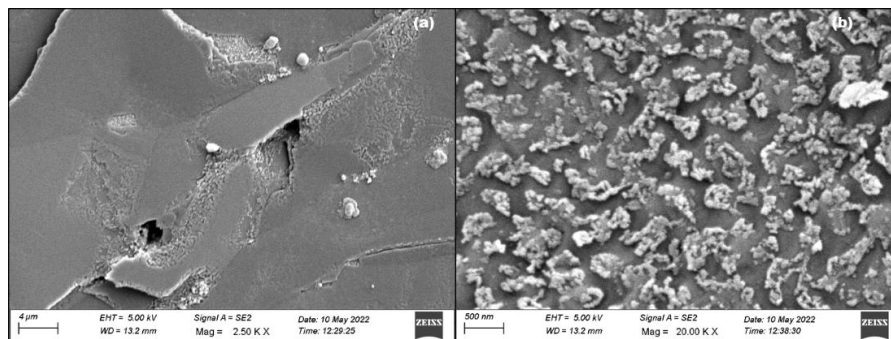
Fig. 1(a&b): represents refined XRD pattern of and synthesis process of thermochromic nature of $(\text{PEA})_2\text{CuCl}_4$.



Crystallographic Information (CIF file) of $(\text{PEA})_2\text{CuCl}_4$ (CCDC No: 892624) was used to refine the powder XRD pattern of synthesised $(\text{PEA})_2\text{CuCl}_4$ using The Full proof Suite program [37, 40]. The optimized values of refinement factors obtained such as chi-square, Bragg R-factor, and RF-factor are 14.5, 16.43, and 10.60 respectively. Refinement confirmed that the material belongs to the $Cmca$ (No: 64) space group in the orthorhombic crystal system with unit cell parameter $a = 38.58 \text{ \AA}$, $b = 7.34 \text{ \AA}$, $c = 7.39 \text{ \AA}$, $\alpha = \beta = \gamma = 90$. Refined structural characteristics of $(\text{PEA})_2\text{CuCl}_4$ is shown in Fig. 1. Planes (002), (004), and (006) are marked in that according to the reflection conditions of $Cmca$ space group.

3.2 Morphological Analysis

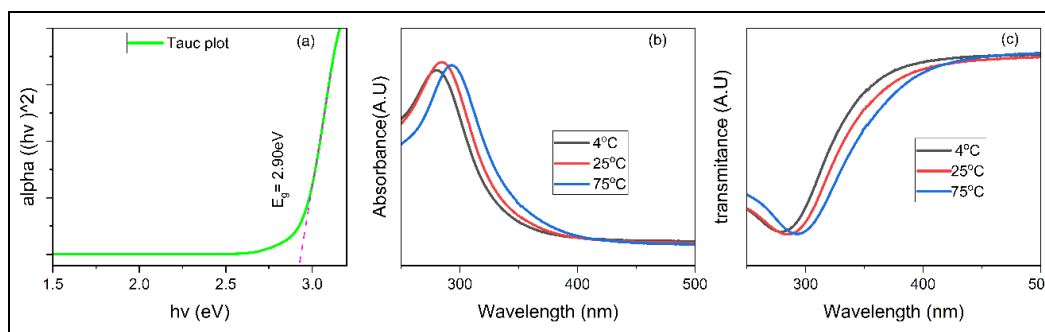
Fig. 2 (a & b): represents FE-SEM micrographs of $(\text{PEA})_2\text{CuCl}_4$ at 2.5KX and 20KX magnification respectively



FE-SEM image of $(\text{PEA})_2\text{CuCl}_4$ film at a magnification of 2.5KX shown in Fig. 2(a) looks like a smooth and continuous one. Upon increasing the magnification to 20KX the clusters and islands formed on the film became visible as shown in fig. 2(b).

3.3 Optical Analysis

Fig. 3 (a b & c) represents Tauc plot, temperature depended UV-Vis absorbance and transmittance analysis respectively

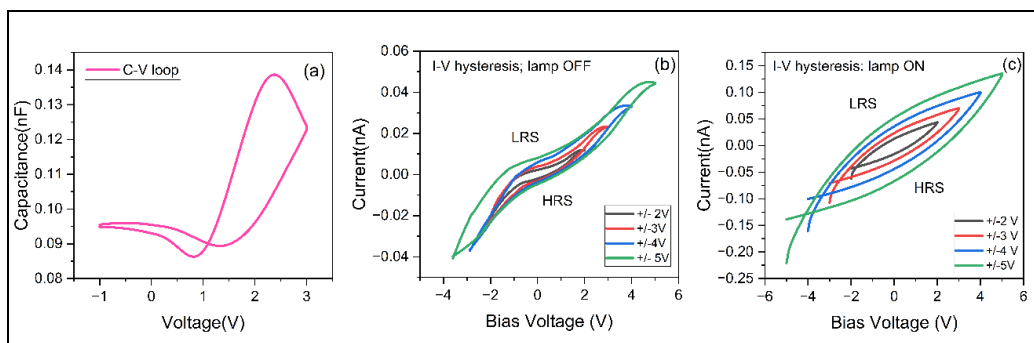


Thin films of $(\text{PEA})_2\text{CuCl}_4$ of thickness 300nm was coated on glass FTO glass substrates and the UV-VIS absorbance spectrum was taken. The obtained data was modified and the Tauc plot was drawn as shown in Fig. 3(a). The nature of the Tauc plot indicates that the synthesized material possesses a direct band gap. The slop drawn at the tailing end touches X-axis at 2.90 eV which is the band gap of the material. During the fabrication of $(\text{PEA})_2\text{CuCl}_4$ thin films show a colour change. During the annealing process, the film shows an orange colour at a temperature on and above 75°C. The colour change from yellow to the orange of $(\text{PEA})_2\text{CuCl}_4$ was shown in Fig .1(b). Upon cooling, the material's colour changed into pale yellow. On repeating the process of heating and cooling the material shows the same effect indicating the reversible thermochromic behaviour of the material [33]. In Fig. 3(b&c), it is clear that as

temperature increases absorbance and transmittance of $(\text{PEA})_2\text{CuCl}_4$ shows a red shift and confirms its thermochromic nature.

3.4 Electrical Analysis

Fig. 4 (a, b & c) represents variation in capacitance and current in $(\text{PEA})_2\text{CuCl}_4$ upon the applied voltage



Electrical properties of $(\text{PEA})_2\text{CuCl}_4$ was analysed via a semiconducting parametric analyser. It results in capacitance(C) and current upon the applied voltage. Capacitance shows a butterfly-shaped switching indicating non-centrosymmetric nature and the presence of ferroelectricity in $(\text{PEA})_2\text{CuCl}_4$. The voltage window was -1 to 3V and the corresponding capacitance produced varied from 0.095nF to 0.135nF with the crossing of the curve at a voltage of 1.1 V at 1KHz frequency. This type of switching in capacitance made the material suitable for non-volatile memory. Voltage-controlled resistance shifts from a high resistance state (HRS) to a low resistance state (LRS) were observable in the I-V characteristics shown in Fig. (b&c). The Resistance switching mechanism present in $(\text{PEA})_2\text{CuCl}_4$ was studied in two environments such as dark and light. The area of the hysteresis loop varies with voltage change, indicating that the charge storage in this material is non-linear. The I-V characteristics of the material show symmetrical behaviour in different sweep voltages; also, the area covered in the loop increases with an increase in the sweep voltage. According to Fig. 4(b), the current values vary between ± 0.04 nA when the lamp is OFF. According to Fig. 4(c), the value of current value was ± 0.15 nA when the lamp was in the ON state. These results confirmed the phot-generated charge carriers support $(\text{PEA})_2\text{CuCl}_4$ to increase the current flow and produce a shift in the positions of HRS and LRS and create an improved switching mechanism.

4. CONCLUSION

In summary, $(\text{PEA})_2\text{CuCl}_4$ was synthesised by a simple solution-based process and morphological analysis confirmed the uniformity of the formed film. The film showed a change in colour from yellow to orange upon heating evidencing thermochromism. This colour change was reversible in nature. Temperature depended on optical analysis shows a red shift in pattern raised upon heating confirming thermochromism. Rietveld

refinement $(\text{PEA})_2\text{CuCl}_4$ is in good accordance with the known crystallographic data. The material is belonged to Cmc_2a space group and possesses a non-centrosymmetric crystal structure and ferroelectric properties. The electrical characteristics indicated that the material is suitable for non-volatile memory applications. Switching between high and low resistance states is visible in current versus voltage characteristics. The same characteristics upon light environment output enhanced the resistance switching behaviour presented in $(\text{PEA})_2\text{CuCl}_4$.

REFERENCES

- Park, N. Perovskite solar cells: an emerging photovoltaic technology. *Materials Today*, 18(2), 65-72.2015
- Xiao, Z., & Yan, Y., Progress in theoretical study of metal halide perovskite solar cell materials. *Advanced Energy Materials*, 7(22), 1701136, 2017
- Yin, W. J., Shi, T., & Yan, Y., Unique properties of halide perovskites as possible origins of the superior solar cell performance. *Advanced Materials*, 26(27), 4653-4658, 2014
- Hsiao, Y. C., Wu, T., Li, M., Liu, Q., Qin, W., & Hu, B. Fundamental physics behind high-efficiency organo-metal halide perovskite solar cells. *J. Mater. Chem. A*, 3(30), 15372-15385, 2015
- Ou, Q., Bao, X., Zhang, Y., Shao, H., Xing, G., Li, X., Shao, L., & Bao, Q., Band structure engineering in metal halide perovskite nanostructures for optoelectronic applications. *NMS*, 1(4), 268-287, 2019
- Umari, P., Mosconi, E., & De Angelis, F. Infrared dielectric screening determines the low exciton binding energy of metal-halide perovskites. *J. Phys. Chem. Lett.*, 9(3), 620-627. 2018
- Liu, Y., Kim, D., Ilevlev, A. V., Kalinin, S. V., Ahmadi, M., Ovchinnikova, O. S., Ferroic Halide Perovskite Optoelectronics. *Adv. Funct. Mater.*, 31, 2102793.2021
- Akihiro Kojima, Kenjiro Teshima, Yasuo Shirai, and Tsutomu Miyasaka, *Journal of the J. Am. Chem. Soc.*, 131 (17), 6050,2009
- Im, J. H., Lee, C. R., Lee, J. W., Park, S. W., & Park, N. G., 6.5% efficient perovskite quantum-dot-sensitized solar cell. *Nanoscale*, 3(10), 4088, 2011
- Yi, C., Li, X., Luo, J., Zakeeruddin, S.M. and Grätzel, M., Perovskite Photovoltaics with Outstanding Performance Produced by Chemical Conversion of Bilayer Mesostructured Lead Halide/TiO₂ Films. *Adv. Mater.*, 28: 2964-2970, 2016
- Feng, W., Lin, K., Li, W., Xiao, X., Lu, J., Yan, C., and Wei, Z., Efficient all-inorganic perovskite light-emitting diodes enabled by manipulating the crystal orientation. *J. Mater. Chem. A*, 9(17), 11064-11072, 2021
- Prasad, M. D., Krishna, M. G., & Batabyal, S. K. Silver Bismuth Iodide Nanomaterials as Lead-Free Perovskite for Visible Light Photodetection. *ACS Appl. Nano Mater.*, 4(2), 1252-1259, 2021
- Ge, S., Huang, Y., Chen, X., Zhang, X., Xiang, Z., Zhang, R., Li, W., Cui, Y., *Adv. Mater. Interfaces*, 6, 1802071, 2019
- Senanayak, S. P., Abdi-Jalebi, M., Kamboj, V. S., Carey, R., Shivanna, R., Tian, T., Siringhaus, H., A general approach for hysteresis-free, operationally stable metal halide perovskite field-effect transistors. *Sci. Adv.*, 6(15), eaaz4948, 2020
- Kostopoulou, A., Vernardou, D., Makri, D., Brintakis, K., Savva, K., Stratakis, E., Highly stable metal halide perovskite microcube anodes for lithium-air batteries. *J. Power Sources*, 3, 100015, 2020

Qin, Y., Gao, F. F., Qian, S., Guo, T. M., Gong, Y. J., Li, Z. G., Bu, X. H., Multifunctional Chiral 2D Lead Halide Perovskites with Circularly Polarized Photoluminescence and Piezoelectric Energy Harvesting Properties. *ACS nano*, 16(2), 3221-3230, 2021

Ren, M., Qian, X., Chen, Y., Wang, T., & Zhao, Y., Potential lead toxicity and leakage issues on lead halide perovskite photovoltaics. *J. Hazard. Mater.*, 426, 127848, 2021

Park, B. W., & Seok, S. I., Intrinsic instability of inorganic–organic hybrid halide perovskite materials. *Adv. Mater.*, 31(20), 1805337, 2019

Zhou, Y., & Zhao, Y., Chemical stability and instability of inorganic halide perovskites. *Energy Environ. Sci.*, 12(5), 1495-1511, 2019

Pathak, A.K., Batabyal, S.K. Formation of 2D-Layered (CH₃NH₃)₃Sb₂I₉ Lead-Free Perovskite Phase from CH₃NH₃I and SbSI: Photodetection Activity in Carbon Based Lateral Devices. *J. Electron. Mater.*, 50, 5989–5994, 2021

Wu, G., Liang, R., Zhang, Z., Ge, M., Xing, G., Sun, G., 2D Hybrid Halide Perovskites: Structure, Properties, and Applications in Solar Cells, *Small* 17, 2103514, 2022

Chen, Y., Sun, Y., Peng, J., Tang, J., Zheng, K., Liang, Z., 2D Ruddlesden–Popper Perovskites for Optoelectronics *Adv. Mater.*, 30, 1703487, 2018

Fu, H., Dion–Jacobson halide perovskites for photovoltaic and photodetection applications. *J. Mater. Chem. C*, 9(20), 6378-6394, 2021

Yuce, H., Perini, C. A., Hidalgo, J., Castro-Méndez, A., Evans, C., Betancur, P. F., Vagott, J. N., An, Y., Bairley, K., Demir, M. M., & Correa-Baena, J., Understanding the impact of SrI₂ additive on the properties of Sn-based halide perovskites. *Opt. Mater.*, 123, 111806, 2022

Chen, G., Wang, P., Wu, Y., Zhang, Q., Wu, Q., Wang, Z., Zheng, Z., Liu, Y., Dai, Y., Huang, B., Lead-Free Halide Perovskite Cs₃Bi₂xSb_{2–2x}I₉ (x ≈ 0.3) Possessing the Photocatalytic Activity for Hydrogen Evolution Comparable to that of (CH₃NH₃)PbI₃. *Adv. Mater.*, 32, 2001344, 2020

Pandey, P., Sharma, N., Panchal, R. A., Gosavi, S. W., & Ogale, S., Realization of High Capacity and Cycling Stability in Pb-Free A₂CuBr₄ (A= CH₃NH₃/Cs, 2 D/3 D) Perovskite-Based Li-Ion Battery Anodes. *ChemSusChem.*, 12(16), 3742-3746. 2016

Chiara, R., Morana, M., & Malavasi, L., Germanium-Based Halide Perovskites: Materials, Properties, and Applications. *ChemPlusChem.*, 86(6), 879-888, 2021

Fu, H., Jiang, C., Luo, C., Lin, H., & Peng, H. (2021). A Quasi-Two-Dimensional Copper Based Organic-Inorganic Hybrid Perovskite with Reversible Thermochromism and Ferromagnetism. *Eur. J. Inorg. Chem.*, (47), 4984-4989. 2021

Bi, C., Wang, S., Li, Q., Kershaw, S. V., Tian, J., & Rogach, A. L., Thermally stable copper (II)-doped cesium lead halide perovskite quantum dots with strong blue emission. *J. Phys. Chem. Lett.*, 10(5), 943-952, 2019

Pareja-Rivera, C., Solis-Ibarra, D., Reversible and Irreversible Thermochromism in Copper-Based Halide Perovskites. *Adv. Optical Mater.*, 9, 2100633, 2021

Pan, Xw., Wu, G., Wang, M. et al. Partially reversible photochromic behavior of organic-inorganic perovskites with copper (II) chloride. *J. Zhejiang Univ. Sci. A*, 10, 710, 2009

Ceng Han, Alasdair J. Bradford, Alexandra M. Z. Slawin, et al., Structural Features in Some Layered Hybrid Copper Chloride Perovskites: ACuCl₄ or A₂CuCl₄ *Inorg. Chem.*, 60 (15), 11014, 2021

Li, J., Liu, X., Cui, P. et al. Lead-free thermochromic perovskites with tunable transition temperatures for smart window applications. *Sci. China Chem.* 62, 1257–1262, 2019

Groeneveld, B. G. H. M., Duim, H., Kahmann, S., De Luca, O., Tekelenburg, E. K., Kamminga, M. E., ... & Loi, M. A., Photochromism in Ruddlesden–Popper copper-based perovskites: a light-induced change of coordination number at the surface. *J. Mater. Chem. C*, 8(43), 15377-15384, 2020

Li, M., Zuo, W. W., Yang, Y. G., Aldamasy, M. H., Wang, Q., Cruz, S. H. T., and Abate, A., Tin halide perovskite films made of highly oriented 2D crystals enable more efficient and stable lead-free perovskite solar cells. *ACS Energy Lett.*, 5(6), 1923-1929, 2020

Conings, B., Drijkoningen, J., Gauquelin, N., Babayigit, A., D'Haen, J., D'Olieslaeger, L., Boyen, H. G., Intrinsic thermal instability of methylammonium lead trihalide perovskite. *Adv. Energy Mater.*, 5(15), 1500477, 2015

Polyakov, Alexey O., Anne H. Arkenbout, Jacob Baas, Graeme R. Blake, Auke Meetsma, Antonio Caretta, Paul HM Van Loosdrecht, and Thomas TM Palstra. "Coexisting ferromagnetic and ferroelectric order in a CuCl₄-based organic-inorganic hybrid." *Chem. Mater.*, 24(1), 133-139, 2012

Albert, A., Sreelekshmi, N., Jinchu, I., Sreelatha, K., Sreekala, C.: Electron trapping action of functionalized carbon nanotubes and PEDOT:PSS nanocomposite in inverted perovskite solar cell. In: *AIP Conf. Proc.*, vol. 2162, p. 020122, 2019

Priya, H., Albert, A., Indiramma, J., Sreelatha, K.S., Sreekala, C.S.N.O.A.: Enhanced moisture stability of perovskite nanostructure using methyl ammonium lead iodide and benzyl ammonium iodide as additive. In: *AIP Conf. Proc.*, vol. 2287, p. 020015, 2020

Rodríguez-Carvajal, Introduction to the program FULLPROF: refinement of crystal and magnetic structures from powder and single crystal data. *Laboratoire Léon Brillouin (CEA-CNRS): Saclay, France*, 2001

Nguyen, C. A., & Lee, P. S, Capacitance-voltage measurement in memory devices using ferroelectric polymer. In *Device and Process Technologies for Microelectronics, MEMS, and Photonics IV (Vol. 6037, pp. 201-208)*.